

## Ultrafast Infrared and UV–Vis Studies of the Photochemistry of Methoxycarbonylphenyl Azides in Solution

Jiadan Xue,<sup>†</sup> Hoi Ling Luk,<sup>†</sup> S. V. Eswaran,<sup>‡</sup> Christopher M. Hadad,<sup>\*,†</sup> and Matthew S. Platz<sup>\*,†</sup><sup>†</sup>Department of Chemistry, The Ohio State University, 100 West 18th Avenue, Columbus, Ohio 43210, United States<sup>‡</sup>St. Stephen's College, University of Delhi, Delhi 110007, India

## Supporting Information

**ABSTRACT:** The photochemistry of 4-methoxycarbonylphenyl azide (**2a**), 2-methoxycarbonylphenyl azide (**3a**), and 2-methoxy-6-methoxycarbonylphenyl azide (**4a**) were studied by ultrafast time-resolved infrared (IR) and UV–vis spectroscopies in solution. Singlet nitrenes and ketenimines were observed and characterized for all three azides. Isoxazole species **3g** and **4g** are generated after photolysis of **3a** and **4a**, respectively, in acetonitrile. Triplet nitrene **4e** formation correlated with the decay of singlet nitrene **4b**. The presence of water does not change the chemistry or kinetics of singlet nitrenes **2b** and **3b**, but leads to protonation of **4b** to produce nitrenium ion **4f**. Singlet nitrenes **2b** and **3b** have lifetimes of 2 ns and 400 ps, respectively, in solution at ambient temperature. The singlet nitrene **4b** in acetonitrile has a lifetime of about 800 ps, and reacts with water with a rate constant of  $1.9 \times 10^8 \text{ L}\cdot\text{mol}^{-1}\cdot\text{s}^{-1}$  at room temperature. These results indicate that a methoxycarbonyl group at either the para or ortho positions has little influence on the ISC rate, but that the presence of a 2-methoxy group dramatically accelerates the ISC rate relative to the unsubstituted phenylnitrene. An *ortho*-methoxy group highly stabilizes the corresponding nitrenium ion and favors its formation in aqueous solvents. This substituent has little influence on the ring-expansion rate. These results are consistent with theoretical calculations for the various intermediates and their transition states. Cyclization from the nitrene to the azirine intermediate is favored to proceed toward the electron-deficient ester group; however, the higher energy barrier is the ring-opening process, that is, azirine to ketenimine formation, rendering the formation of the ester–ketenimine (**4d'**) to be less favorable than the isomeric MeO–ketenimine (**4d**).

## 1. INTRODUCTION

Arylnitrenes have been extensively studied by nanosecond laser flash photolysis (LFP),<sup>1,2</sup> nanosecond<sup>3</sup> and picosecond<sup>4</sup> time-resolved Raman spectroscopy (TR<sup>3</sup>), nanosecond time-resolved infrared (TR-IR), and by matrix isolation spectroscopy.<sup>5,6</sup> As a result, a great deal has been learned about their lifetimes and the rate constants of their bimolecular reactions. It is well established that photolysis of aryl azides **1a** (Scheme 1) in solution usually proceeds by extrusion of molecular nitrogen and the release of a singlet aryl nitrene **1b**, that can form a triplet nitrene **1e** by intersystem crossing (ISC) or generate a ketenimine **1d** through a two-step, ring-expansion reaction through azirine **1c**.<sup>7,8</sup> Certain singlet aryl nitrenes can be protonated to form aryl nitrenium ions **1f** in the presence of proton donors, such as water or alcohols (Scheme 2). Most aryl nitrenes, in solution at ambient temperature, isomerize to form a ketenimine rather than undergo ISC to the ground triplet state, but substituent effects on phenylnitrene chemistry can have a huge influence on the reaction rates of these three processes. For example, a substituent at the para position, especially an electron-donating group, can dramatically increase the ISC rate.<sup>9</sup>

Substitution at the ortho position has a large impact on the rate of the ring-expansion reaction.<sup>9</sup> A single ortho substituent usually has little influence on the rate of singlet phenylnitrene isomerization to the azirine. Singlet 2-methylphenylnitrene, at room temperature, has a 1 ns lifetime,<sup>1</sup> the same as that of the parent singlet phenylnitrene. The 2-methyl group directs cyclization to benzazirine away from the substituent for steric reasons. Singlet 2-cyanophenylnitrene<sup>10,11</sup> and 2-acetylphenylnitrene<sup>12</sup> bear sterically undemanding ortho substituents. In these two systems, ring-expansion products are formed both by cyclization away from and toward the substituent.

A di-ortho substituent pattern can exert a dramatic steric effect on azirine formation and prolongs the lifetime of the singlet nitrene. Singlet 2,6-dimethylphenylnitrene, for example, has a lifetime of 13 ns.<sup>1</sup>

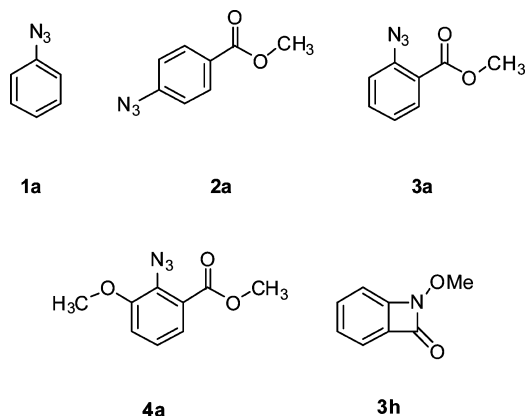
The electronegativity of ortho substituent(s) can also have a large effect on the lifetimes of singlet nitrenes. A single *ortho*-fluoro substituent(s) increases the barrier for ring expansion by  $\sim 1\text{--}3 \text{ kcal/mol}$  relative to the unsubstituted system;<sup>13,14</sup> thus,

Received: September 21, 2011

Revised: May 7, 2012

Published: May 8, 2012

Scheme 1



the singlet 2-fluorophenylnitrene has a lifetime of 8 ns.<sup>13</sup> Fluorine substituents at both ortho positions extend the lifetime of singlet 2,6-difluorophenylnitrene to 240 ns.<sup>13,15</sup> Theory has shown that the electron-withdrawing fluorine substituent makes the adjacent carbon very positively charged, and the positive–positive charge interaction between the *ortho*-carbon and the carbon bearing nitrogen increases the activation barrier from nitrene to azirine.

Phenylnitrenes with functional groups at the *ortho* position can interact to produce a class of azacyclic compounds,<sup>16</sup> such as 2-biphenyl azide, which produces carbazole in excellent yield.<sup>17</sup> Upon photolysis of the 2-methoxycarbonylphenyl azide in a matrix at 10 K, Tomioka et al.<sup>18</sup> observed *N*-methoxyacetinone **3h** with a carbonyl stretch at 1857 cm<sup>-1</sup>, and this acetinone **3h** can be photochemically converted to iminoketenes with the observed C=C=O stretches at 2118 and 2088 cm<sup>-1</sup>.

To our knowledge, there have not been many previous studies of phenylnitrenes substituted with *ortho*-ester groups. As azido esters are widely used as polyfunctional reagents for labeling applications, we sought to learn how this substituent influences the ISC rate of the singlet nitrene, and how the steric and substitution combination would affect the rates for ring expansion or ketenimine formation.

Ultrafast time-resolved UV–vis and infrared spectroscopies are effective methods for the study of excited states and reactive intermediates with short lifetimes. They have been utilized to directly characterize the excited states of aryl azides<sup>19</sup> and some short-lived singlet and triplet nitrenes,<sup>20</sup> ketenimines,<sup>21</sup> and

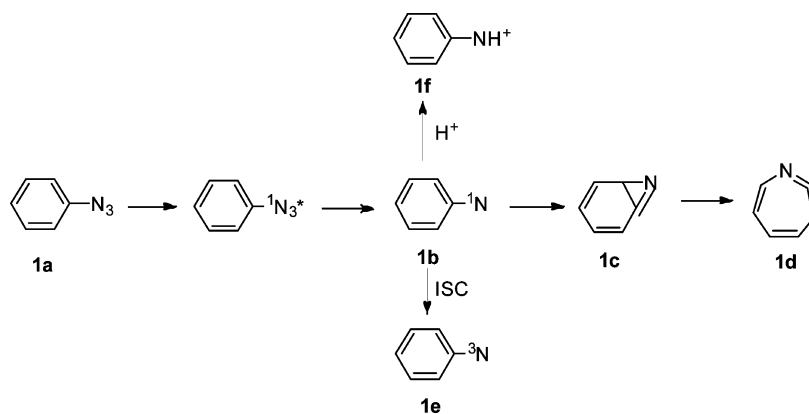
arylnitrenium ions.<sup>5</sup> In this study, we applied ultrafast UV–vis and infrared absorption spectroscopies to study the photochemistry of 4-methoxycarbonylphenyl azide **2a**, 2-methoxycarbonylphenyl azide **3a**, and 2-methoxy-6-methoxycarbonylphenyl azide **4a** in organic and aqueous solutions at room temperature. The carbonyl group imparts reactive intermediates with strong IR vibrations so that one can hope to directly observe and identify singlet and triplet nitrenes, ketenimine, and isoxazole species as well as the corresponding nitrenium ions while also monitoring their formation rates or lifetimes in different solvents.

## 2. EXPERIMENTAL AND COMPUTATIONAL METHODS

**2.1. Synthesis.** 2- and 4-Methoxycarbonylphenyl azides were synthesized from the corresponding commercially available amines according to the standard method of Tomioka.<sup>22</sup>

**2.1.1. 2-Methoxy-6-methoxycarbonylphenyl azide.** To a solution of 1.00 g (5.98 mmol) of 2-amino-3-methoxybenzoic acid in 25 mL of methanol was added 5 mL of concentrated sulfuric acid. The reaction mixture was heated under reflux for 40 h. The cooled reaction mixture was added with sodium bicarbonate solution until the effervescence ceased. The organic material was extracted with dichloromethane (2 × 100 mL) and washed with brine (50 mL) and water (50 mL). The extract was dried over anhydrous MgSO<sub>4</sub> and filtered, and the solvent was removed under reduced pressure to give 1.0 g (92%) of 2-methoxy-6-methoxycarbonylphenylamine as a yellowish brown liquid. To a solution of 1.00 g (5.52 mmol) of 2-methoxy-6-methoxycarbonylphenylamine in 12 mL of tetrahydrofuran was added a mixture of concentrated hydrochloric acid (3 mL) and water (24 mL). The reaction mixture was stirred for 15 min in an ice–methanol bath, and a solution of 609 mg (8.83 mmol) of NaNO<sub>2</sub> in 10 mL of water was added dropwise to the solution, keeping the temperature of the reaction below 5 °C. The reaction mixture was stirred for 15 min at 0 °C and excess nitrous acid was removed by the addition of urea. To the cooled reaction mixture was added dropwise a solution of 857 mg (8.83 mmol) of NaN<sub>3</sub> in 11 mL of water. After the addition was complete, the reaction mixture was stirred for 1 h at room temperature. The organic material was extracted with dichloromethane, and the extract was washed with dilute hydrochloric acid (0.1 M) and dried over anhydrous Na<sub>2</sub>SO<sub>4</sub>. The solvent was removed under reduced pressure to give an orange crude product. The residue was developed on a silica gel column with

Scheme 2. General Reaction Pathways for Arylnitrenes



2.5:9 (dichloromethane/ethyl acetate/hexane) giving 762 mg (67%) of 2-methoxy-6-methoxycarbonylphenylazide as a yellow liquid (frozen to solid in refrigerator):  $^1\text{H}$  NMR (400 MHz,  $\text{CDCl}_3$ )  $\delta$  3.94 (s, 3H), 3.92 (s, 3H) 7.04 (dd,  $J = 1, J = 8$ , 1H), 7.13 (t,  $J = 8$ , 1H), 7.36 (dd,  $J = 2, J = 8$ , 1H).  $^{13}\text{C}$  NMR (400 MHz,  $\text{CDCl}_3$ )  $\delta$  168.7, 147.1, 141.8, 122.5, 114.6, 112.9, 110.1, 55.72, 51.5. HRMS (ESI)  $m/z$  calcd for  $\text{C}_9\text{H}_9\text{N}_3\text{O}_3$  ( $M - \text{Na}^+$ ), 207.0644; found, 207.0612.

**2.2. Ultrafast Spectroscopy.** The ultrafast UV–vis broadband and ultrafast infrared absorption measurements were performed using the home-built spectrometers at The Ohio State University for Chemical and Biophysical Dynamics. These instruments have been described in detail elsewhere.<sup>19,23</sup>

The sample solutions were prepared to provide absorption at the excitation wavelength to be  $\sim 1$  (0.5 and 1 mm spacers for ultrafast IR and UV–vis experiments, respectively).

**2.3. Computational Methods.** Geometry optimizations and transition state searches were performed using the 6-31+G(d,p)<sup>24,25</sup> basis set in conjunction with the B3LYP<sup>26,27</sup> method or the 6-31G\*<sup>28</sup> basis set in conjunction with the complete active space self-consistent field (CASSCF) method.<sup>29,30</sup> The CASSCF calculations used a 10-electron, 10-orbital active space, hereafter designated (10,10) for all species. The ten orbitals comprised the eight orbitals included in the active space, and these are analogous to those used in similar calculations on species involved in the ring expansion of phenylnitrenes,<sup>31</sup> along with the bonding and antibonding orbitals ( $\pi$ ,  $\pi^*$ ) of the C=O bond in the ester group. The nature of all stationary points, either minima or transition states, was determined by calculating the vibrational frequencies at either the B3LYP/6-31+G(d,p) or CASSCF(10,10)/6-31G\* level. The unscaled frequencies were used to obtain corrections for zero-point vibrational energies. For DFT calculations, we have employed unrestricted B3LYP methods and found broken-symmetry solutions for the open-shell singlet nitrenes and the corresponding transition states for azirine formation, as has been described in the literature.<sup>32</sup> The effects of dynamic electron correlation<sup>33</sup> were determined by CASPT2 calculations<sup>34,35</sup> using either 6-31G\* or Dunning's correlation-consistent polarized valence double- $\zeta$  basis set (cc-pVDZ),<sup>36</sup> while using the CASSCF(10,10)/6-31G\* optimized geometries. All calculations were performed using the Gaussian09<sup>37</sup> and MOLCAS version 7.4<sup>38</sup> software packages.

### 3. RESULTS AND DISCUSSION

**3.1. Ultrafast Time-Resolved Infrared Spectroscopic Results for 4-Methoxycarbonylphenyl Azide.** Ultrafast laser flash photolysis (LFP) of 4-methoxycarbonylphenyl azide **2a** in acetonitrile (MeCN) with 270 nm light produces the transient IR spectra in the 1920–1830  $\text{cm}^{-1}$  region shown in Figure 1. The band observed is easily recognized as a 1,2-didehydroazepine (ketenimine) absorption.<sup>39–41a</sup> Inspection of Figure 1 shows that the initially detected vibrational band is broad, then sharpens and blue-shifts over the initial 30 ps. This is consistent with previous reports that hot singlet nitrenes can isomerize to hot benzazirines and then to the thermally excited ketenimines, which then undergo vibrational relaxation.<sup>21</sup> There are only a few direct observations of benzazirines<sup>41b,c</sup> because their barrier to ring-opening is rather small.<sup>31,41d</sup> The kinetics of the ketenimine formation was monitored at 1888  $\text{cm}^{-1}$ , and the decay was fit with a biexponential function, yielding time constants of  $\sim 15$  ps (41%) and  $\sim 2200$  ps (59%). These values correspond to the vibrational cooling

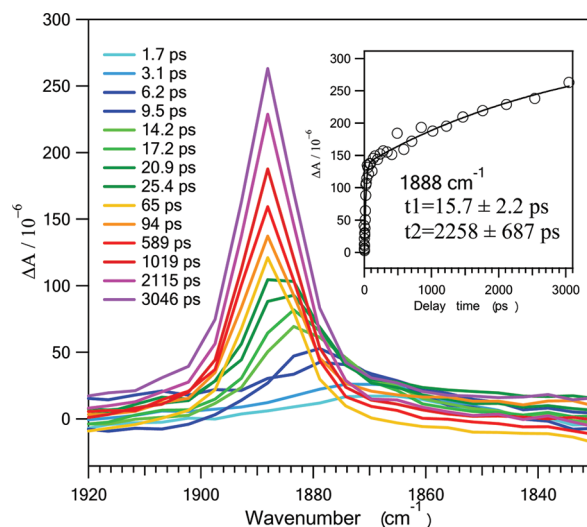


**Figure 1.** Transient IR spectra produced after ultrafast photolysis of 4-methoxycarbonylphenyl azide **2a** in MeCN. The spectra were generated by ultrafast LFP ( $\lambda_{\text{ex}} = 270$  nm) and recorded over a time window of 1–3000 ps. (Inset) Kinetic growth at 1888  $\text{cm}^{-1}$  as fit by a biexponential function.

(VC)<sup>19,20,42–45</sup> of hot ketenimine formed in the reaction of hot singlet nitrene and to the formation of the ketenimine via relaxed singlet nitrene/benzazirine, respectively.

Figure 2 presents transient IR spectra in the 1780–1660  $\text{cm}^{-1}$  region obtained under the same conditions as those of Figure 1. A broad band with a maximum at 1697  $\text{cm}^{-1}$  was detected immediately after the laser pulse, shown as the spectrum obtained at 0.7 ps delay time; this band narrows, and its intensity increases slightly within 3 ps of the laser pulse (Figure 2A). Then, this 1697  $\text{cm}^{-1}$  band blue-shifts to 1701  $\text{cm}^{-1}$  over 17 ps. Finally, the 1701  $\text{cm}^{-1}$  band decays with a time constant of  $\sim 2000$  ps to give a new band at 1714  $\text{cm}^{-1}$  with a clear isosbestic point at 1708  $\text{cm}^{-1}$ , shown in Figure 2C. The 1697–1701  $\text{cm}^{-1}$  band is the carbonyl stretch of the hot and the thermally relaxed singlet nitrene **2b**, and the band narrowing and blue shift can be attributed to a mixture of VC, solvent reorganization,<sup>46</sup> and ring expansion of the hot singlet nitrene. The new band, with a maximum at 1714  $\text{cm}^{-1}$ , partly overlaps with the bleaching of the carbonyl band of the ground state azide. This effect artificially distorts the appearance of the 1722  $\text{cm}^{-1}$  bleaching to appear (incorrectly) as a recovery at post delay times. The 1714  $\text{cm}^{-1}$  positive band observed in Figure 2C is the ester carbonyl stretch of the ketenimine, and its formation can be fitted with the same time constant as the carrier of the characteristic C=C=N stretching at 1888  $\text{cm}^{-1}$  displayed in Figure 1. Although density functional theory (DFT, B3LYP) calculations predict that the singlet nitrene (**2b**), triplet nitrene (**2e**), and ketenimine (**2d**) have rather similar carbonyl stretching frequencies, there is no evidence for the formation of a second species formed as the singlet nitrene is decaying. To our knowledge, this is the first direct observation of a singlet aryl nitrene using time-resolved infrared spectroscopy.

Analogous ultrafast time-resolved infrared experiments were performed with the 4-methoxycarbonylphenyl azide **2a** in MeCN:D<sub>2</sub>O (1:1) mixed aqueous solvent, and the spectra are presented in the Supporting Information. The ultrafast infrared experimental results demonstrate that the presence of water has

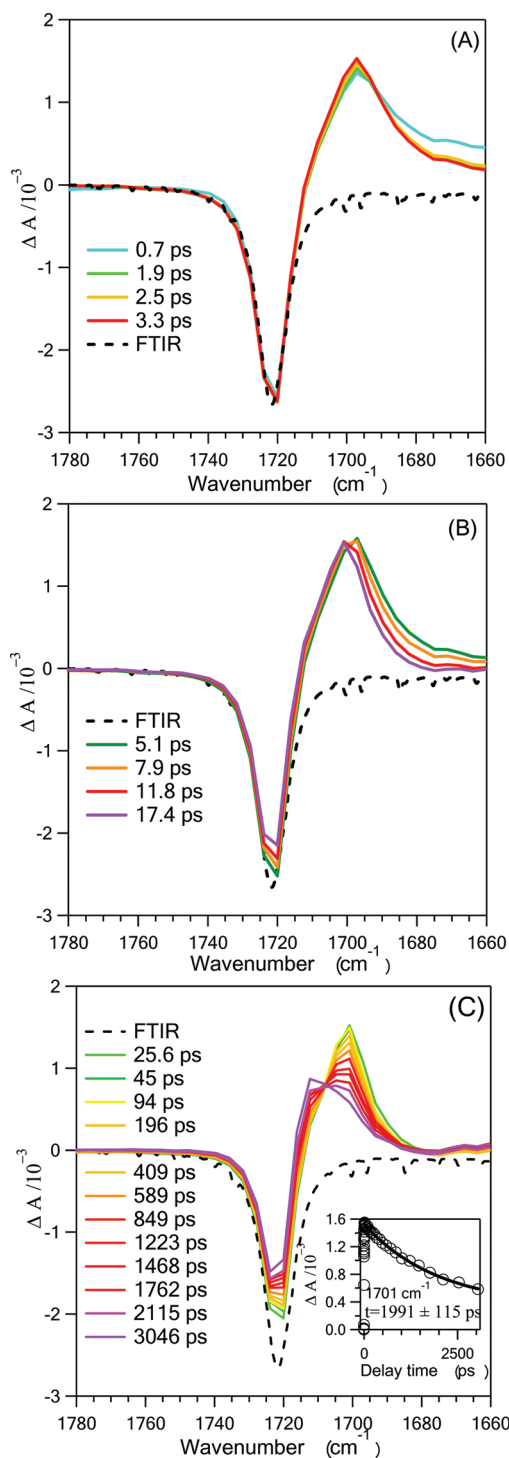


**Figure 2.** Transient IR spectra produced after ultrafast photolysis of 4-methoxycarbonylphenyl azide **2a** in MeCN. The spectra were generated by ultrafast LFP ( $\lambda_{\text{ex}} = 270$  nm) recorded over time windows of 0.7–3.3 ps (A), 5.1–17.4 ps (B), and 25.6–3046 ps (C). Kinetic decay at  $1701$   $\text{cm}^{-1}$  as fit by an exponential function (C inset).

no influence on the chemistry and the kinetics of singlet nitrene **2b**.

**3.2. Ultrafast Time-Resolved Infrared Spectroscopic Results for 2-Methoxycarbonylphenyl Azide.** Ultrafast LFP of 2-methoxycarbonylphenyl azide **3a** with 270 nm excitation in neat MeCN and in MeCN/D<sub>2</sub>O (2:1) mixed aqueous solvent generates ketenimine **3d** with a time constant

of  $\sim 400$  ps in each solvent system. The transient infrared spectra recorded in the  $1920$ – $1830$   $\text{cm}^{-1}$  region and the associated kinetic information are presented in the Supporting Information. As with azide **2a**, the IR spectrum of photo-generated ketenimine **3d** shows a characteristic C=C=N stretching band at  $1883$   $\text{cm}^{-1}$ , and the kinetics can be fit to a biexponential function, reflecting the VC of hot ketenimine and formation of the ketenimine via relaxed singlet nitrene/benzazirine, respectively.

Figure 3 displays the ultrafast IR spectra recorded in the  $1770$ – $1670$   $\text{cm}^{-1}$  region upon 270 nm excitation of 2-methoxycarbonylphenyl azide **3a** in MeCN. The IR spectra obtained in the MeCN/D<sub>2</sub>O (2:1) mixed aqueous solvent are presented in the Supporting Information. The hot singlet nitrene **3b** is generated immediately after the laser pulse as depicted in the transient absorption spectrum recorded 0.7 ps after the laser pulse. The hot singlet nitrene then undergoes VC to form the relaxed singlet nitrene **3b**, and both species contribute to the generation of a new carbonyl vibrational band at  $1715$   $\text{cm}^{-1}$  as displayed in Figure 3B at various postexcitation delays. The kinetics of the new band formation were monitored at  $1715$   $\text{cm}^{-1}$  and fit using a biexponential function with time constants of  $\sim 9$  ps (52%) and  $\sim 430$  ps (48%). By analogy to the transient IR spectra observed in the same region after LFP photolysis of the azide **2a**, the growing  $1715$   $\text{cm}^{-1}$  band in Figure 3B is assigned to the ketenimine. This result is in agreement with the spectra of hot and relaxed ketenimine obtained in the  $1880$   $\text{cm}^{-1}$  region. We expect both ketenimine isomers to be formed based on calculations to be discussed later.

In addition to ketenimine, a second new species is formed near  $1640$   $\text{cm}^{-1}$  as shown in Figure 4. The carrier of this signal has a lifetime of more than 3 ns. Examination of Figure 4 shows that this new species was generated in a very hot state immediately after the laser pulse, and that the new species is largely produced from the hot singlet nitrene. The new band at  $1640$   $\text{cm}^{-1}$  was observed only upon LFP of 2-methoxycarbonylphenyl azide **3a** and 2-methoxy-6-methoxycarbonylphenyl azide **4a** (vide infra) but not with 4-methoxycarbonylphenyl azide **2a**. This leads us to conclude that the new species absorbing at  $1640$   $\text{cm}^{-1}$  is isoxazole **3g** (Scheme 3). By applying a scaling factor<sup>47</sup> of 0.9648, our DFT calculations predict that this isoxazole type species **3g** has a scaled IR frequency at  $1631$   $\text{cm}^{-1}$ , corresponding to the C=C stretching mode in the 5-membered ring, with a strong intensity (see Supporting Information for details). This prediction is in excellent agreement with the experimental IR result. The new species **3g** was also observed in the MeCN/D<sub>2</sub>O (2:1) mixed aqueous solvent with the same formation kinetics as that observed in neat MeCN.

**3.3. Ultrafast Time-Resolved Infrared Spectroscopic Results for 2-Methoxy-6-methoxycarbonylphenyl Azide.** Ultrafast LFP of 2-methoxy-6-methoxycarbonylphenyl azide **4a** with 272 nm excitation in neat MeCN produces the isoxazole **4g** and the ketenimine **4d**. The transient infrared spectra and kinetic information are presented in the Supporting Information. As was found with 2-methoxycarbonylphenyl azide, an isoxazole species **4g** is formed as evidenced by a band at  $1645$   $\text{cm}^{-1}$ . In order to confirm the presence of isoxazole, steady-state infrared spectra were recorded before and after photolysis (Figure S5, Supporting Information). The growth of the absorption at  $1632$   $\text{cm}^{-1}$  after photolysis further supports the formation of isoxazole species **4g**.

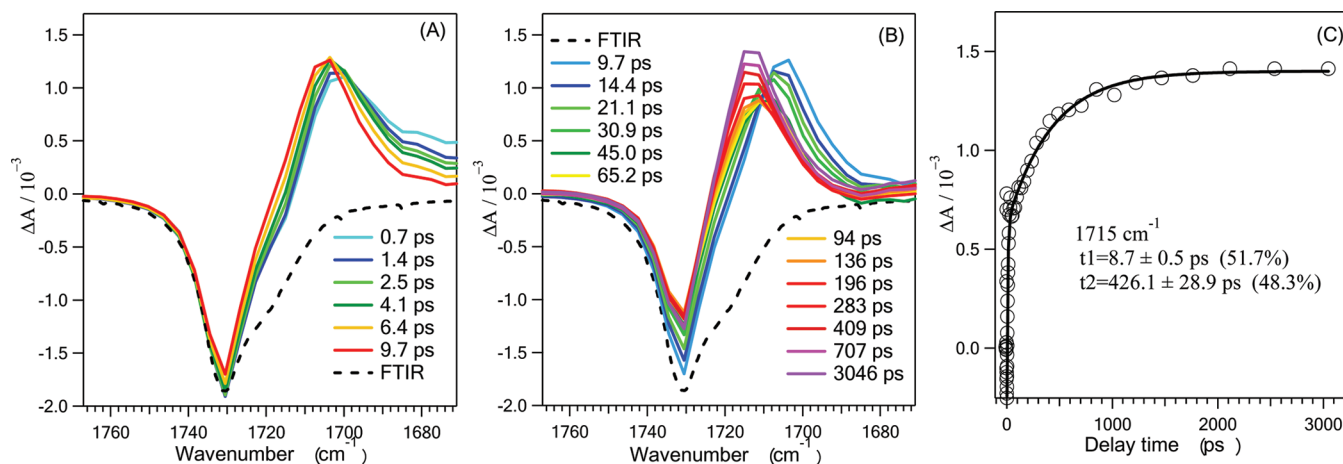


**Figure 3.** Transient IR spectra produced after ultrafast photolysis of 2-methoxycarbonylphenyl azide **3a** in MeCN. The spectra were generated by ultrafast LFP ( $\lambda_{\text{ex}} = 270$  nm) over a time window of 0.7–9.7 ps (A), 9.7 ps–3046 ps (B), and kinetic growth at 1715  $\text{cm}^{-1}$  and fitting with a biexponential function (C).

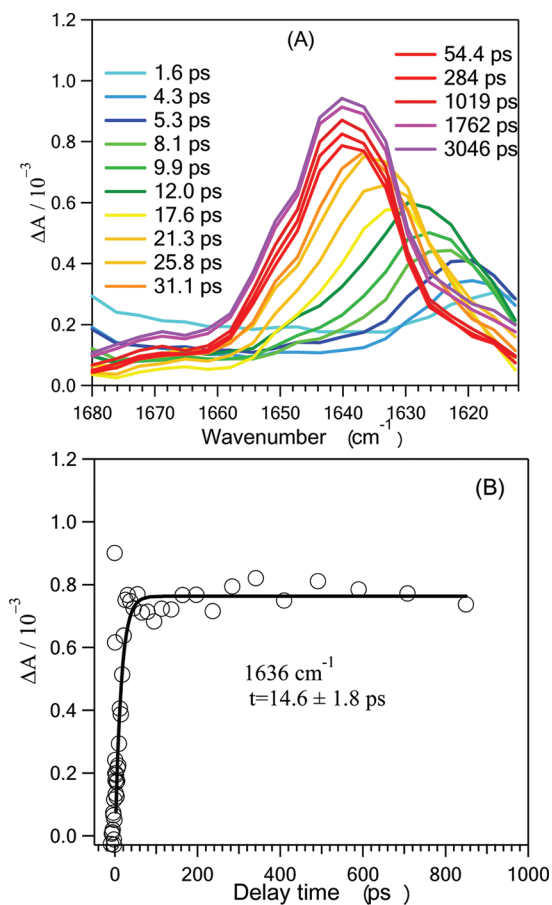


**Figure 4.** Transient IR spectra and the kinetics at 1636  $\text{cm}^{-1}$  produced after 270 nm ultrafast photolysis of 2-methoxycarbonylphenyl azide **3a** in MeCN.

The ketenimine has a characteristic  $\text{C}=\text{C}=\text{N}$  stretching band at 1880  $\text{cm}^{-1}$ , and its formation kinetics can be fit with a biexponential function reflecting the VC of the hot ketenimine ( $\sim 12$  ps, 54%) and formation of the ketenimine via relaxed singlet nitrene/benzazirine ( $\sim 800$  ps, 46%), respectively. The ketenimine has a lifetime of more than 3 ns under these experimental conditions.

The transient IR spectra observed in the 1780–1660  $\text{cm}^{-1}$  region after photolysis of azide **4a** in MeCN shows one distinct difference compared to the data obtained with azides **2a** and **3a** in the same solvent. As shown in Figure 5B, a third new band at 1755  $\text{cm}^{-1}$ , which is at a higher IR frequency than the azide bleach at 1730  $\text{cm}^{-1}$ , is formed with the same time constant ( $\sim 800$  ps) as the singlet nitrene **4b** (1700  $\text{cm}^{-1}$ ) decays. The new species at 1755  $\text{cm}^{-1}$  is tentatively assigned to triplet nitrene **4e** rather than the other possible ketenimine isomer or its benzazirine analogue because theory predicts that ring expansion toward the ester group has a very large activation barrier (vide infra). This assignment is also in agreement with the DFT predicted (and scaled) IR frequencies of triplet nitrene **4e** (1708  $\text{cm}^{-1}$ ) as this species was found to have a slightly higher IR frequency than the azide bleach predicted at 1707  $\text{cm}^{-1}$  at the same level of theory.

Assuming these assignments are valid, we deduce that the singlet nitrene **4b** undergoes both ring expansion and ISC in MeCN to form the ketenimine and the triplet nitrene, respectively. This interpretation postulates that the 2-methoxy group accelerates the ISC rate relative to unsubstituted singlet phenylnitrene,<sup>2</sup> in the same manner as does a *para*-methoxy substituent.<sup>9</sup>

We cannot exclude the possibility that the carrier of the 1755  $\text{cm}^{-1}$  band is a benzazirine in an unusually deep minimum as both benzazirine **4c'** and triplet nitrene **4e** give the same predicted carbonyl stretch at 1708  $\text{cm}^{-1}$ . We prefer the triplet nitrene as our tentative assignment since observations of benzazirines are quite rare.<sup>4b,c</sup> Moreover, as mentioned previously, it seems reasonable to expect that an *ortho*-methoxy group to accelerate ISC in a manner similar to that of a *para*-methoxy group.<sup>9</sup>

Similar ultrafast IR experiments were performed in MeCN/ $\text{D}_2\text{O}$  (1:1) with azide **4a**, and the spectra recorded in the 1780–1660  $\text{cm}^{-1}$  region are shown in Figure 6. The positive band at 1690  $\text{cm}^{-1}$ , detected at early delay times (Figure 6A), is assigned to singlet nitrene **4b**, and the absorption band blue-shifts within the initial 15 ps due to VC. While the singlet nitrene band is decaying, a positive band at 1700  $\text{cm}^{-1}$  rises and with an isosbestic point at 1704  $\text{cm}^{-1}$ . This 1700  $\text{cm}^{-1}$  band cannot be assigned to the corresponding ketenimine since the 1880  $\text{cm}^{-1}$  band is not generated with this azide (**4a**), in the presence of water, upon laser photolysis. We assign this new

Scheme 3

2. X=4-methoxycarbonyl  
3. X=2-methoxycarbonyl  
4. X=2-methoxy-6-methoxycarbonyl

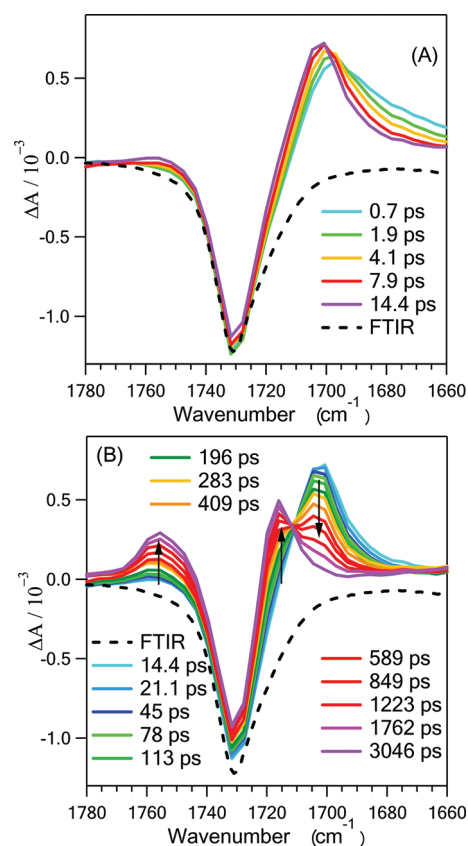
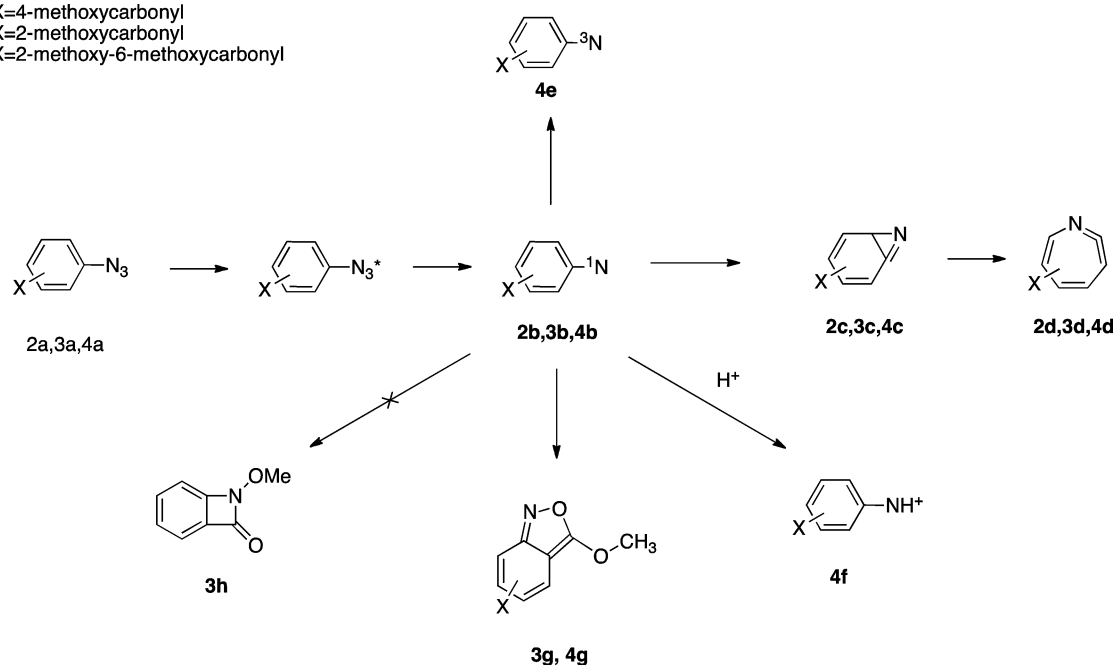


**Figure 5.** Transient IR spectra produced after ultrafast photolysis of 2-methoxy-6-methoxycarbonylphenyl azide **4a** in MeCN. The spectra were generated by ultrafast LFP ( $\lambda_{\text{ex}} = 270 \text{ nm}$ ) recorded over a time window of 0.7–14.4 ps (A) and 14.4–3046 ps (B).

species to nitrenium ion **4f** because the nitrenium ion was observed and characterized in the ultrafast UV–vis experiments (see below for details). DFT calculations predicted that the

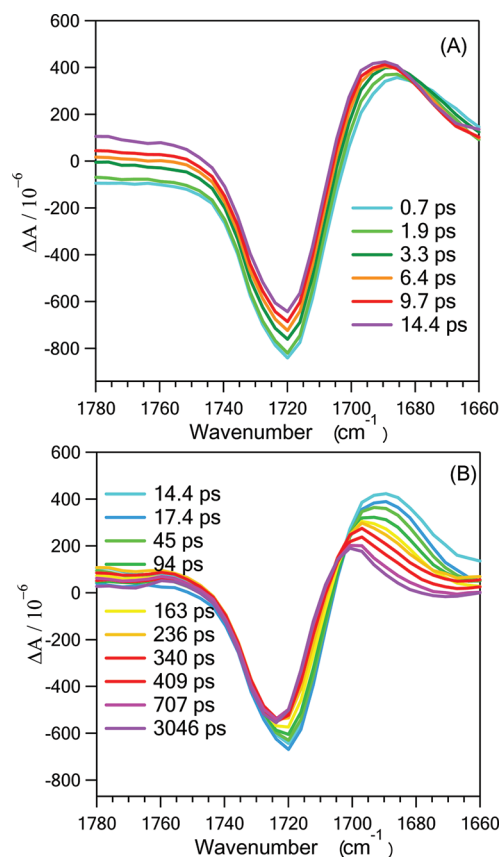


**Figure 6.** Transient IR spectra produced after ultrafast photolysis of 2-methoxy-6-methoxycarbonylphenyl azide **4a** in MeCN/D<sub>2</sub>O (1:1). The spectra were generated by ultrafast LFP ( $\lambda_{\text{ex}} = 270 \text{ nm}$ ) with a time window of 0.7–14.4 ps (A) and 14.4–3046 ps (B).

nitrenium ion **4f** has a scaled carbonyl stretching band at  $1737 \text{ cm}^{-1}$  with a calculated strong intensity. The production of the nitrenium ion accelerates the decay of singlet nitrene **4b**,

monitored at  $1693\text{ cm}^{-1}$ , and fit to an exponential function with a decay time constant of  $\sim 400\text{ ps}$ . Less triplet nitrene **4e** is generated in the presence of water as only a low intensity characteristic band is present at  $1755\text{ cm}^{-1}$  in Figure 6B.

**3.4. Ultrafast UV–Vis Spectroscopic Results with 2-Methoxy-6-methoxycarbonylphenyl Azide.** Ultrafast LFP ( $\lambda_{\text{ex}} = 313\text{ nm}$ ) of 2-methoxy-6-methoxycarbonylphenyl azide **4a** in MeCN produces the transient UV–vis spectra shown in Figure 7. The first species detected is observed immediately

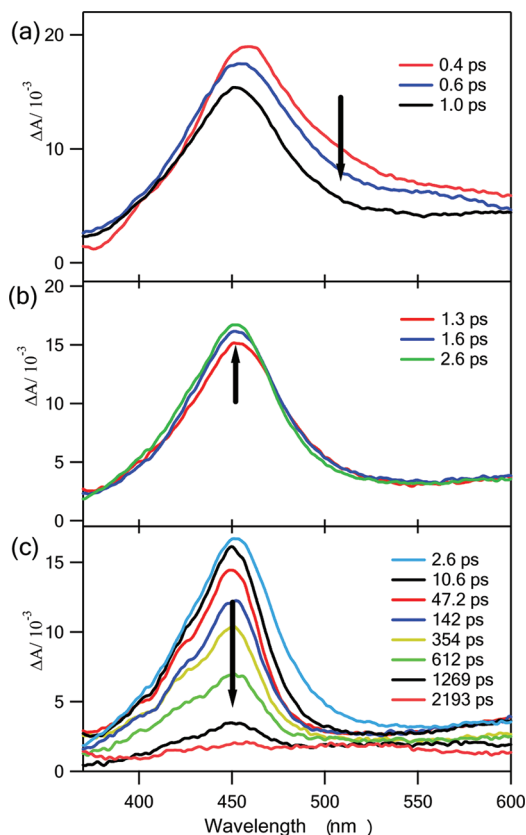


**Figure 7.** Transient UV–vis spectra obtained by the photolysis of 2-methoxy-6-methoxycarbonylphenyl azide **4a** in MeCN. Spectra were produced by ultrafast LFP ( $\lambda_{\text{ex}} = 313\text{ nm}$ ) with a time window of (a) 0.4–1.0 ps, (b) 1.3–2.6 ps, and (c) 10.6–2200 ps.

after the laser pulse, at 460 nm. The absorption maximum blue shifts within 1 ps. This species is attributed to the  $S_1$  state of azide **4a**. This also agrees with the predictions of time-dependent density functional theory (TD-DFT, details below) that 313 nm light excites the azide to its  $S_1$  state. As the  $S_1$  state of azide **4a** decays, a transient absorption spectrum attributed to the singlet nitrene **4b** grows in at 450 nm. Between 1 and 10 ps, after the laser pulse, the transient absorption band of the singlet nitrene grows and narrows due to solvation<sup>48</sup> and VC.<sup>42–45</sup> The relaxed singlet nitrene has a lifetime of  $747 \pm 100\text{ ps}$  in MeCN consistent with the  $\sim 800\text{ ps}$  time constant obtained in ultrafast IR experiment for the singlet nitrene **4b**.

Figure 8 presents the ultrafast time-resolved UV–vis spectra recorded in a MeCN/ $\text{H}_2\text{O}$  (3:1) mixed aqueous solvent system after LFP ( $\lambda_{\text{ex}} = 313\text{ nm}$ ) of azide **4a**. As in MeCN, in the mixed aqueous solvent, the  $S_1$  state of the azide is generated immediately after the laser pulse and decays within 1 ps to produce the singlet nitrene. In contrast to the results obtained in MeCN, the singlet nitrene decay in the mixed solvent

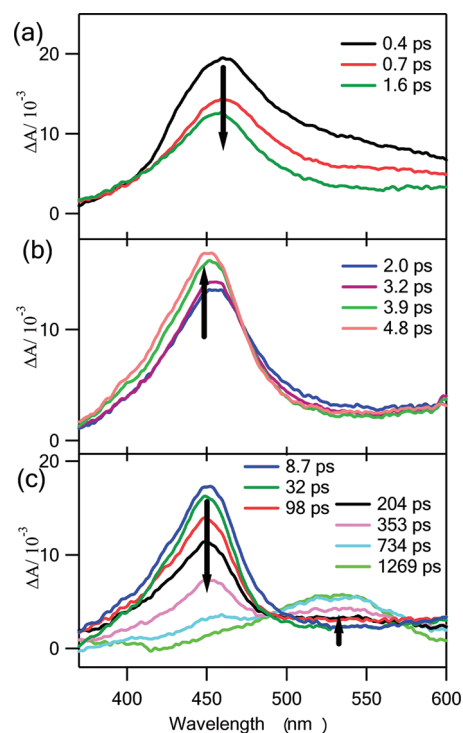


**Figure 8.** Transient UV–vis spectra obtained by the photolysis of 2-methoxy-6-methoxycarbonylphenyl azide **4a** in MeCN/ $\text{H}_2\text{O}$  (3:1). Spectra were produced by ultrafast LFP ( $\lambda_{\text{ex}} = 313\text{ nm}$ ) recorded over a time window of (a) 0.4–1.6 ps, (b) 2.0–4.8 ps, and (c) 8.7–1200 ps.

produces a new absorption band at 530 nm. The band grows with an isosbestic point at 490 nm and a time constant of  $429 \pm 54\text{ ps}$ . This transient has a lifetime longer than our instrumental limit (3 ns). On the basis of McClelland and co-workers, studies of para substituted phenyl azide by nanosecond LFP,<sup>49–52</sup> the new transient species produced in aqueous solvent is assigned to the singlet nitrenium ion, in good agreement with TD-DFT calculations in water that predict that the nitrenium ion **4f** has a maximum absorption at 531 nm.

Similar experiments were performed for the azide in MeCN/ $\text{H}_2\text{O}$  as a mixed aqueous solvent, in different proportions, and the ultrafast UV–vis spectra are shown in the Supporting Information. As the content of water increases from 25% to 50% in solution, the nitrenium ion forms more rapidly with a time constant of  $\sim 400\text{ ps}$  in 25% aqueous solution to  $\sim 200\text{ ps}$  in 50% aqueous solution. The pseudo first-order rate constant of formation of the nitrenium ion was plotted as a function of the water concentration as shown in Figure 10S, Supporting Information, and well fit to a linear function, so that the first-order rate constant for the singlet nitrene **4b** toward water  $k_{[\text{H}_2\text{O}]}$  was found to be  $1.9 \times 10^8\text{ L}\cdot\text{mol}^{-1}\cdot\text{s}^{-1}$ .

**3.5. Ketanimine Assignment and Calculations of the Activation Barrier to Singlet Nitrene Ring Expansion.** To aid in understanding the experimental results obtained with these nitrenes and the assignment of the different species observed, we performed a series of calculations on the two-step, ring-expansion reactions for the corresponding nitrenes using both density functional theory (DFT)<sup>26,27</sup> and complete active space self-consistent field (CASSCF)<sup>29,30</sup> with second-order perturbation theory (CASPT2) corrections.<sup>34,35</sup> These results provide an overall view of the energetics of the ring expansion process for methoxycarbonylarylnitrenes. We remind the reader that singlet phenylnitrene has a preferred open-shell config-

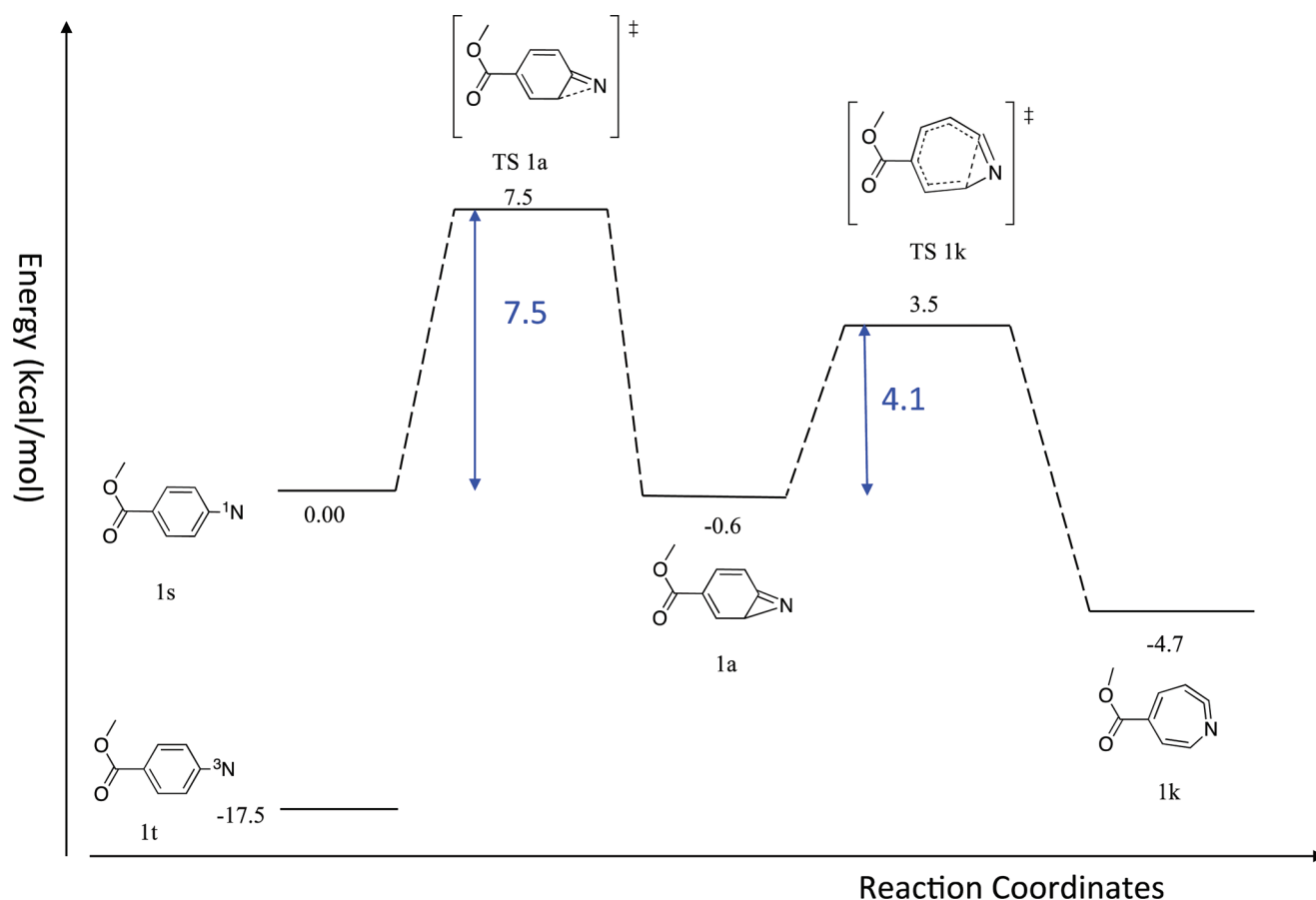


**Figure 9.** Relative energy profile (in kcal/mol) obtained from CASPT2/cc-pVDZ//CASSCF(10,10)/6-31G\* calculations for ketenimine formation from 4-methoxycarbonylphenylnitrene (**2b** → **2d**).

uration, and CASSCF methods, while challenging for determining the ideal or most practical active space, provide greater confidence for an accurate description of the open-shell nitrene.

For singlet 4-methoxycarbonylphenylnitrene **2b** at the CASPT2/cc-pVDZ//CASSCF(10,10)/6-31G\* level of theory (Figure 9), we found an activation barrier of 7.5 kcal/mol to form the ketenimine, which is comparable to that of unsubstituted phenylnitrene. However, for singlet 2-methoxycarbonylphenylnitrene **3b** (Figure 10), the activation barrier for cyclization to form the azirine is much smaller (2–3 kcal/mol). A possible reason for this result is the decreased stability of the singlet *ortho*-methoxycarbonylphenylnitrene **3b** relative to that of *para*-singlet nitrene **2b**. For both singlet nitrenes, the carbonyl group prefers to be in plane with the phenyl ring to achieve higher conjugation and stability. However, when the carbonyl group is in the *ortho* position, this results in severe repulsion between the nitrene nitrogen and the carbonyl oxygen. Hence, it is found that the CASPT2 energy for *ortho*-singlet nitrene **3b** is 4.5 kcal/mol higher than that of *para*-**2b**. This increase in energy of the singlet nitrene decreases the activation energy barrier to cyclization to form azirine. This also explains why the cyclization of **3b** to form azirine **3c** is much faster than the unsubstituted singlet nitrene **1b** as moving the nitrene nitrogen out of plane relieves steric repulsion through cyclization.

From the CASPT2 results, it is likely that both isomeric ketenimines are formed from the *ortho*-methoxycarbonyl substituted singlet phenylnitrene. Unfortunately, IR spectroscopy

cannot distinguish between these two ketenimines by either vibrational frequency or kinetics, due to their very similar infrared vibrations (less than 20 cm<sup>-1</sup> difference). The energy barriers to formation of the two isomers are predicted to be similar; thus, their rates of formation are expected to be similar.

Let us now discuss the potential energy surface for 2-methoxy-6-methoxycarbonylphenylnitrene, **4b**, which has two *ortho* substituents: a methoxy and a methoxycarbonyl moiety on phenylnitrene. For the singlet nitrene **4b**, the ring-expansion reaction can proceed either toward or away from the ester group and produce two ketenimine isomers as shown in Figure 11. (In Figure 13S, Supporting Information, we also present the relative energy profiles obtained from B3LYP/6-31+G(d,p) and CASPT2(10,10)/6-31G\*//B3LYP/6-31+G(d,p) calculations. Additional figures and computational details are provided in the Supporting Information.) The CASPT2/6-31G\*//CASSCF(10,10)/6-31G\* calculations predict that the ester-ketenimine (**4d'**) is less stable than the MeO-ketenimine (**4d**) and that the latter is 9.9 kcal/mol lower in energy than the ester-ketenimine (**4d'**). Similar to the case of 2-methoxycarbonylphenylnitrene **2b**, the activation barrier is small for the cyclization step. However, the barrier for ring-opening to form ester-ketenimine (**4d'**) is extremely high (13.5 kcal/mol). This would lead us to the conclusion that MeO-ketenimine (**4d**) would be the only possible ketenimine formed at room temperature. In order to confirm the accuracy of the potential energy surface's topology, CASPT2 single-point energy calculations were performed on the B3LYP/6-31+G(d,p) optimized geometries, and these results are shown in Figure

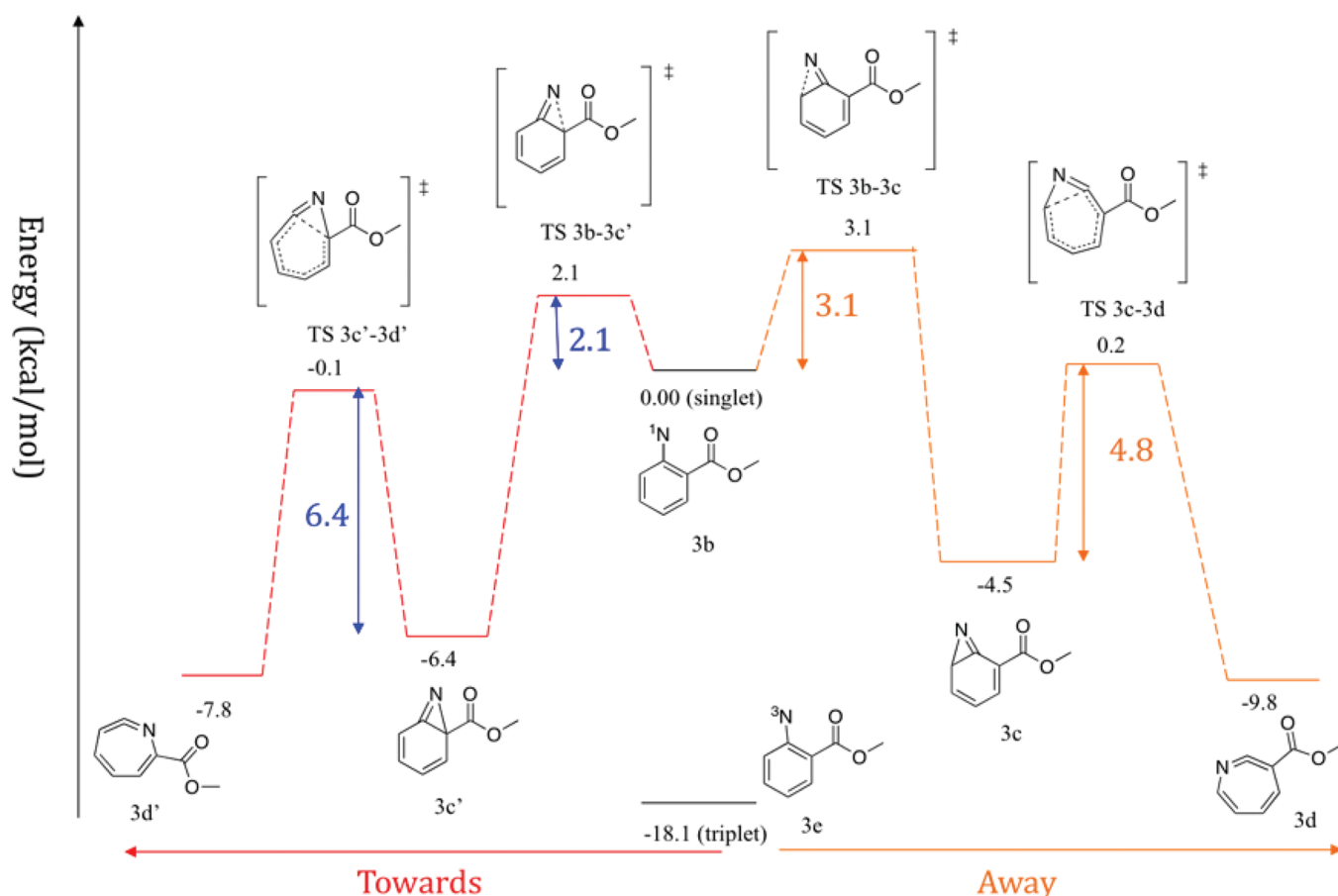


**Figure 10.** Relative energy profile (in kcal/mol) obtained from CASPT2//cc-pVDZ//CASSCF(10,10)/6-31G\* calculations of ketenimine formation from 2-methoxycarbonylphenylnitrene ( $3b \rightarrow 3d$ ).

13S, Supporting Information. The CASPT2 calculations are consistent with each other and independent of a B3LYP or CASSCF geometry. The different topology observed with the B3LYP energies can be attributed to spin contamination of the singlet (open-shell) nitrene and the transition states for azirine formation. We did attempt CASPT2 calculations with the cc-pVDZ basis set, as described earlier for 2-methoxycarbonyl and 4-methoxycarbonylphenylnitrene; however, those attempts failed due to challenges in defining the correct active spaces for the singlet nitrene and the transition states for azirine formation. Nevertheless, since the azirines, the ketenimines, and their transition states are well described by a closed-shell description, we also used higher level CBS-QB3<sup>53</sup> calculations (see Supporting Information, Table 34S) to provide accurate values for the conversion of azirine to ketenimine. At the CBS-QB3 level of theory, the activation barrier for conversion of the ester–azirine ( $4c'$ ) to the ester–ketenimine ( $4d'$ ) is large (9.1 kcal/mol), while the corresponding barrier is only 0.4 kcal/mol to go from the MeO–azirine ( $4c$ ) to the MeO–ketenimine ( $4d$ ). These results are consistent across the various levels of theory: B3LYP (9.0 vs 1.3 kcal/mol), CASPT2//CASSCF (13.5 vs 2.2 kcal/mol), and CASPT2//B3LYP (12.1 vs 2.5 kcal/mol), respectively.

Usually, cyclization of a phenylnitrene to a benzazirine is much slower than a subsequent ring-opening of the benzazirine to ketenimine. However, the increase in energy of the singlet nitrene changes the topology of the potential energy surface describing the formation of ketenimine. In the *ortho* substituted system, cyclization to form azirine is no longer

the rate-determining step; instead, azirine formation by insertion toward the methoxy group leads to subsequent ring-expansion and ketenimine formation ( $4d$ ) as the preferred kinetic and thermodynamic product.

B3LYP predictions of the IR frequencies are in good agreement with the assignment of the ketenimine species  $4d$  observed in the ultrafast IR spectrum displayed in Table 1. The calculation of MeO–ketenimine ( $4d$ ) shows that this species has strong infrared vibrations at 1866 and 1705  $\text{cm}^{-1}$ , and this result is consistent with the experimentally observed ultrafast IR spectra in which two positive vibration bands were observed at 1880 and 1716  $\text{cm}^{-1}$ .

The calculations predict that benzazirine  $4c'$  is the kinetic product and exists in a relatively deep energy minimum. Thus, it is possible that this species is the carrier of the 1755  $\text{cm}^{-1}$  band and not the triplet nitrene. Given that we are decomposing the azide precursor with 270 nm light, we expect and observe that singlet nitrene  $4b$  is formed with substantial excess vibrational energy. Thus, we hypothesize that  $4b$  has sufficient energy to explore the potential energy surface and find a pathway to the thermodynamic, singlet state product ketenimine  $4d$ . Thus, we tentatively assign the carrier of the 1755  $\text{cm}^{-1}$  band to the global minimum, the triplet nitrene. We also prefer this assignment because of the expectation that an *ortho*-methoxy substituent will accelerate ISC in the same manner as a *para*-methoxy group.<sup>9</sup>

**3.6. Influence of Ester and Methoxy Substituents on the Singlet Nitrene.** Distinct from a single *ortho*- or *para*-methyl or fluorine substituent, which have similar effects on the

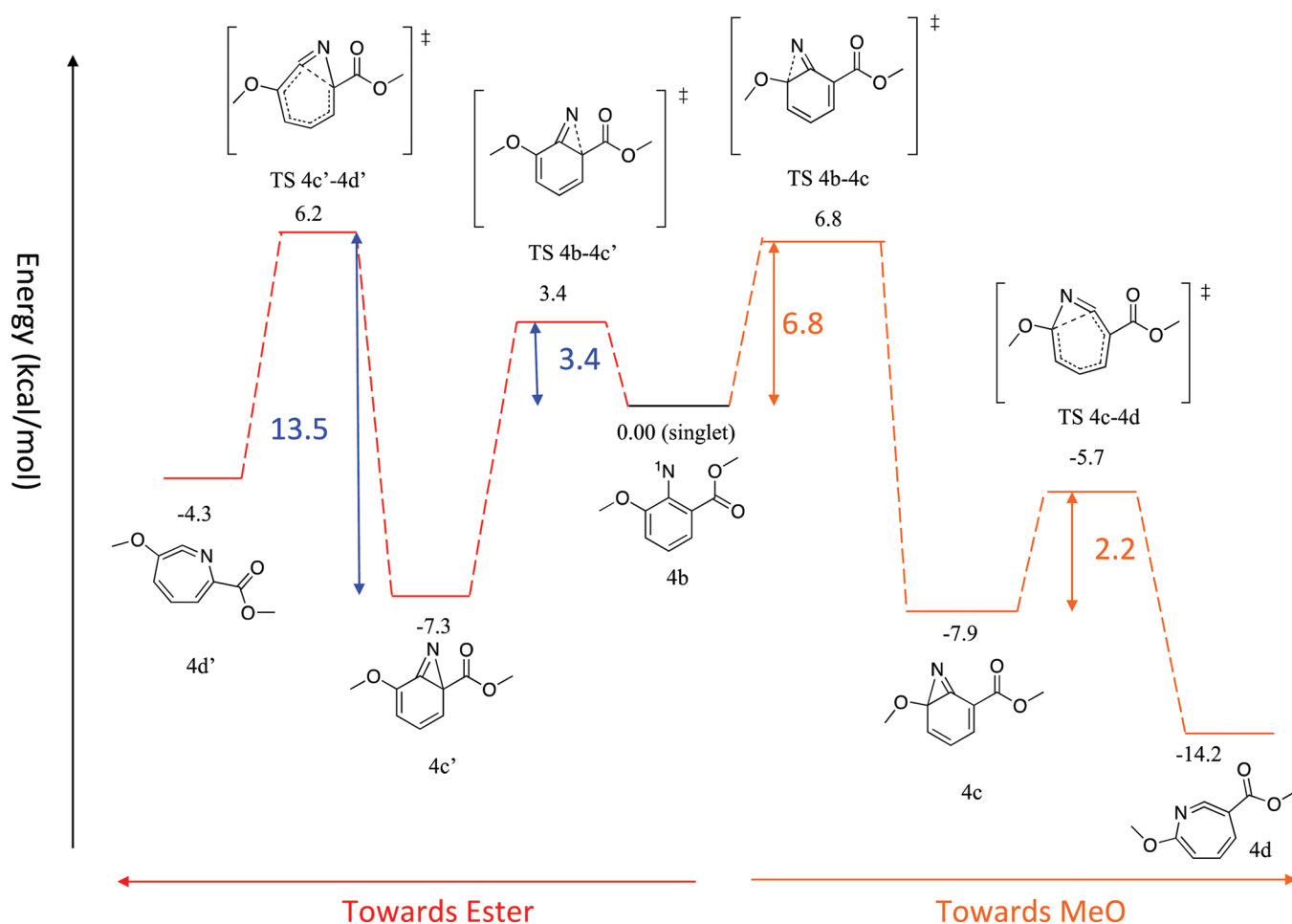


**Figure 11.** Relative energy profile (in kcal/mol) obtained for ketenimine formation from 2-methoxy-6-methoxycarbonylphenylnitrene (**4b** → **4d**) at the CASPT2/6-31G\*\*//CASSCF(10,10)/6-31G\* level of theory.

**Table 1.** DFT Calculation on Predicted Vibrational Frequencies and IR Intensities for the MeO–Ketenimine (**4d**) and Ester–Ketenimine (**4d'**) (Scaling Factor = 0.9648)

	frequencies (cm <sup>-1</sup> )	IR intensity (km/mol)	vibration descriptions
MeO–ketenimine ( <b>4d</b> )	1866	376	C=C=N stretching
	1705	443	C=O stretching
ester–ketenimine ( <b>4d'</b> )	1862	64	C=C=N stretching
	1703	255	C=O stretching

ring-expansion rate of a singlet phenyl nitrene, the ester group has a very different influence on the ring expansion of the singlet nitrenes depending on whether it is positioned at the para or ortho position. For example, singlet 4-methoxycarbonylphenylnitrene **2b** forms the ketenimine with a time constant of 2200 ps, while we observe a 400 ps time constant for the 2-methoxycarbonyl analogue. These experimental results are consistent with the predictions of theory. CASPT2 calculations predict that the activation barrier to form ketenimine is 7.5 kcal/mol and 2–3 kcal/mol for 4-methoxycarbonyl- and 2-methoxycarbonylphenylnitrenes, respectively. This difference can be attributed to the greater ability of the carbonyl group to localize the electron in the nonbonding  $\pi$  orbital at the *ortho*-carbon to which the substituent is attached. This explanation has been proposed previously by Gritsan and co-workers<sup>11</sup> following study of the 2-, 3-, and 4-cyano-substituted singlet

phenylnitrenes. In that study, the 4-cyano phenylnitrene was found to have a slower cyclization rate than the 2-cyano phenylnitrene. The cyclization at a substituted 2-carbon is much faster when the substituent is cyano, rather than methyl or fluoro.<sup>11</sup>

The ultrafast IR and UV–vis experimental results show that the lifetime of relaxed 2-methoxy-6-methoxycarbonylphenyl singlet nitrene **4b** is  $\sim 800$  ps in MeCN at room temperature. This lifetime is similar to that of the parent singlet phenylnitrene,  $\sim 1$  ns, in solution at room temperature, but the parent lifetime is controlled by benzazirine formation and not ISC, which has a rate constant (determined at low temperature) of  $\sim 10^6$  s<sup>-1</sup>.<sup>2</sup> On the basis of our spectroscopic assignments, we posit that both the triplet nitrene and the ketenimine are formed, while the relaxed singlet nitrene **4b** decays. In this interpretation, the ISC rate for **4b** must be much faster than the ISC rate of parent phenylnitrene ( $3.2 \times 10^6$  s<sup>-1</sup>),<sup>2</sup> determined at low temperature, and comparable to that found previously with 4-methoxyphenylnitrene, which was estimated to be greater than  $5 \times 10^8$  s<sup>-1</sup> by laser flash photolysis measurements.<sup>9</sup> We propose that the 2-methoxy group promotes a large acceleration of the ISC rate as it increases the zwitterionic character of the singlet nitrene relative to the parent system, which facilitates a spin–orbit coupling mechanism of ISC.<sup>54</sup>

Ketenimine formation rate was estimated to be  $(0.1–1.2) \times 10^9$  s<sup>-1</sup>, which is similar to that of parent and 2-methyl and di-

*ortho*-methyl substituted analogues, but faster than the di-*ortho*-fluoro substituted phenylnitrene.<sup>13</sup> The fast formation rate of ketenimine deduced from ultrafast IR experiments indicates that the di-*ortho* substituent pattern examined here has little influence on the rate of ketenimine formation. However, the ester group has a large directing effect on cyclization that is steric in nature. Ring expansion for the singlet 2-methoxy-6-methoxycarbonylphenylnitrene greatly prefers cyclization toward the methoxy group rather than the ester group.

The ultrafast IR data and the theoretical calculation results demonstrate that MeO–ketenimine (**4d**) is more stable and formed more rapidly than the ester–ketenimine (**4d'**). However, our CASPT2 calculations (Figure 11) showed that cyclization to benzazirine is faster toward the electron-deficient ester group, and these theoretical results are consistent with the previous cyano-substituted singlet phenylnitrene study<sup>11</sup> by Gritsan et al. However, in our case, the calculated higher energy barrier in the second step of ring-opening, that is, azirine to ketenimine formation, renders the formation of the ester–ketenimine (**4d'**) to be unfavorable. Hence, we predict that the MeO–ketenimine (**4d**) is formed in preference to the ester–ketenimine (**4d'**) and interpret the time-resolved data accordingly.

**3.7. Photochemistry of 2-Methoxycarbonylphenyl Azide and the Formation of Isoxazole.** Tomioka<sup>18</sup> and co-workers did not observe the formation of isoxazole **3g** in their low temperature, matrix-isolation spectroscopy study of the photochemistry of 2-methoxycarbonylphenyl azide. The observation of the 1640 cm<sup>-1</sup> band, however, by ultrafast time-resolved IR spectroscopy in this article provides evidence for the formation of the isoxazole **3g**. Another reason for the assignment of the 1640 cm<sup>-1</sup> IR band to isoxazole **3g** rather than azetinone **3h** is that the 1857 cm<sup>-1</sup> (C=O stretching in **3h**<sup>18</sup>) IR band was not observed upon 270 nm laser pulse photolysis of azide **3a** in MeCN and in mixed aqueous solution. Moreover, there was no evidence for the existence of imino ketenes species formation by photointerconversion from azetinone<sup>18</sup> in our fs time-resolved IR experiments on photolysis of azide **4a** in MeCN.

The absence of detection of azetinone **3h** is in agreement with the results of Sun et al.<sup>55</sup> This group, using nanosecond IR spectroscopy, detected ketenimine as the only intermediate (on the microsecond time scale) in *n*-heptane at room temperature. Thus, we conclude that, at room temperature, the singlet nitrene **3b** decays by producing the ketenimines **3d** (**3d'**) and isoxazole **3g**, respectively.

From calculations, we predict that there is an activation barrier of 10.5 kcal/mol (CASPT2/cc-pVDZ//CASSCF(10,10)/6-31G\*) to form the isoxazoles. This large activation barrier explains why we only observe the formation of the isoxazole from vibrationally hot singlet nitrenes, while only ketenimines are formed from the vibrationally relaxed singlet nitrene.

In contrast to the CASPT2 calculations, DFT calculations predict a much lower activation energy barrier (2.7 kcal/mol) to isoxazole formation. The discrepancy can be attributed to the failure to accurately consider the open-shell nature of the singlet nitrene. The related isoxazole can be formed from **4b** with an activation barrier of 9.3 kcal/mol (CASPT2/cc-pVDZ//CASSCF(10,10)/6-31G\*).

## 4. CONCLUSIONS

As shown in Scheme 3, 270 nm laser photolysis of 4- and 2-methoxycarbonylphenyl and 2-methoxy-6-methoxycarbonylphenyl azides generate singlet nitrenes from initial excitation to the azide S<sub>n</sub> (*n* > 1) excited state. The initially formed singlet nitrenes are born vibrationally excited. Singlet nitrene **2b** has a lifetime of 2 ns in MeCN and in mixed aqueous solvent at room temperature. Singlet nitrene **3b** produces the ketenimine and isoxazole **3g**, with a time constant of 400 ps in solution. Singlet nitrene **4b**, in MeCN, produces ketenimine by ring expansion toward the methoxy group and isoxazole **4g** by reaction with the carbonyl oxygen. On the basis of DFT calculations and the behavior of 4-methoxyphenylnitrene,<sup>9</sup> we propose that singlet nitrene **4b** rapidly forms triplet nitrene **4e** as well. These results demonstrate that the methoxycarbonyl group at both the para and ortho positions have little influence on the ISC rate. In water containing solvent systems, most of the singlet nitrene **4b** formed in solution is protonated to produce nitrenium ion **4f**. The ortho methoxy group stabilizes the nitrenium ion and accelerates its formation in the presence of water, but has little influence on the ring-expansion rate.

## ■ ASSOCIATED CONTENT

### Supporting Information

Ultrafast IR and UV–vis spectra, kinetic data with the fitted curve discussed herein, additional computational data, Cartesian coordinates for the geometries of all species, and full references of 37 and 38. This material is available free of charge via the Internet at <http://pubs.acs.org>.

## ■ AUTHOR INFORMATION

### Corresponding Author

\*Phone: 614-688-3141. Fax: 614-292-1685. E-mail: [platz.1@osu.edu](mailto:platz.1@osu.edu) (M.S.P.); [hadad.1@osu.edu](mailto:hadad.1@osu.edu) (C.M.H.).

### Notes

The authors declare no competing financial interest.

## ■ ACKNOWLEDGMENTS

The ultrafast experiments were performed at the Ohio State Center for Chemical and Biophysical Dynamics, established with the generous support of the National Science Foundation. The Ohio Supercomputer Center generously provided computational resources. Support of this work by the National Institutes of Health (R01-GM073666) is gratefully acknowledged.

## ■ REFERENCES

- (1) Gritsan, N. P.; Gudmundsdottir, A. D.; Tigelaar, D.; Platz, M. S. *J. Phys. Chem. A* **1999**, *103*, 3458–3461.
- (2) Gritsan, N. P.; Zhu, Z.; Hadad, C. M.; Platz, M. S. *J. Am. Chem. Soc.* **1999**, *121*, 1202–1207.
- (3) Xue, J.; Du, Y.; Chuang, Y. P.; Phillips, D. L.; Wang, J.; Luk, H. L.; Hadad, C. M.; Platz, M. S. *J. Phys. Chem. A* **2008**, *112*, 1502–1510.
- (4) Kwok, W. M.; Chan, P. Y.; Phillips, D. L. *J. Phys. Chem. B* **2004**, *108*, 19068–19075.
- (5) Wang, J.; Burdzinski, G.; Zhu, Z.; Platz, M. S.; Carra, C.; Bally, T. *J. Am. Chem. Soc.* **2007**, *129*, 8380–8388.
- (6) Morawietz, J.; Sander, W. *J. Org. Chem.* **1996**, *61*, 4351–4354.
- (7) Lwowski, W. *Nitrenes*; Wiley: New York, 1970.
- (8) Scriven, E. F. V. *Azides and Nitrenes*; Academic Press: New York, 1984.
- (9) (a) Gritsan, N. P.; Tigelaar, D.; Platz, M. S. *J. Phys. Chem. A* **1999**, *103*, 4465–4469. (b) Gritsan, N. P.; Platz, M. S. Photochemistry of

Azides: the Azide/Nitrene Interface. In *Organic Azides: Syntheses and Applications*; Bräse, S., Banert, K., Eds.; John Wiley & Sons, Ltd.: West Sussex, U.K., 2010; pp 311–364.

(10) Lamara, K.; Redhouse, A. D.; Smalley, R. K.; Thompson, J. R. *Tetrahedron* **1994**, *50*, 5515–5526.

(11) Gritsan, N. P.; Likhovorik, I.; Tsao, M.-L.; Celebi, N.; Platz, M. S.; Karney, W. L.; Kemnitz, C. R.; Borden, W. T. *J. Am. Chem. Soc.* **2001**, *123*, 1425–1433.

(12) Berwick, M. A. *J. Am. Chem. Soc.* **1971**, *93*, 5780–5786.

(13) Gritsan, N. P.; Gudmundsdottir, A. D.; Tigelaar, D.; Zhu, Z.; Kahley, M. J.; Hadad, C. M.; Platz, M. S. *J. Am. Chem. Soc.* **2001**, *123*, 1951–1962.

(14) Karney, W. L.; Borden, W. J. *J. Am. Chem. Soc.* **1997**, *119*, 3347–3350.

(15) Mandel, S.; Liu, J.; Hadad, C. M.; Platz, M. S. *J. Phys. Chem. A* **2005**, *109*, 2816–2821.

(16) Wentrup, C. *Adv. Heterocycl. Chem.* **1981**, *28*, 231–361.

(17) Smith, P. A. S.; Brown, B. B. *J. Am. Chem. Soc.* **1951**, *73*, 2435–2437.

(18) Tomioka, H.; Ichikawa, N.; Komatsu, K. *J. Am. Chem. Soc.* **1993**, *115*, 8621–8626.

(19) Burdzinski, G.; Hackett, J. C.; Wang, J.; Gustafson, T. L.; Hadad, C. M.; Platz, M. S. *J. Am. Chem. Soc.* **2006**, *128*, 13402–13411.

(20) Wang, J.; Kubicki, J.; Burdzinski, G.; Hackett, J. C.; Gustafson, T. L.; Hadad, C. M.; Platz, M. S. *J. Org. Chem.* **2007**, *72*, 7581–7586.

(21) Burdzinski, G.; Middleton, C. T.; Gustafson, T. L.; Platz, M. S. *J. Am. Chem. Soc.* **2006**, *128*, 14804–14805.

(22) Murata, S.; Abe, S.; Tomioka, H. *J. Org. Chem.* **1997**, *62*, 3055–3061.

(23) Wang, J.; Burdzinski, G.; Platz, M. S. *J. Am. Chem. Soc.* **2008**, *130*, 11195–11209.

(24) Clark, T.; Chandrasekhar, J.; Spitznagel, G. W.; Schleyer, P. V. R. *J. Comput. Chem.* **1983**, *4*, 294–301.

(25) Frisch, M. J.; Pople, J. A.; Binkley, J. S. *J. Chem. Phys.* **1984**, *80*, 3265–3269.

(26) Becke, A. D. *J. Chem. Phys.* **1993**, *98*, 5648–5652.

(27) Lee, C.; Yang, W.; Parr, R. G. *Phys. Rev. B* **1988**, *37*, 785–789.

(28) Hariharan, P. C.; Pople, J. A. *Theor. Chim. Acta* **1973**, *28*, 213–222.

(29) Roos, B. O. *Adv. Chem. Phys.* **1987**, *69*, 339–445.

(30) Roos, B. O. *Int. J. Quantum Chem. Symp.* **1980**, *14*, 175–189.

(31) Karney, W. L.; Borden, W. T. *J. Am. Chem. Soc.* **1997**, *119*, 1378–1387.

(32) Johnson, W. T. G.; Sullivan, M. B.; Cramer, C. J. *Int. J. Quantum Chem.* **2001**, *85*, 492–508.

(33) Moller, C.; Plesset, M. S. *Phys. Rev.* **1934**, *46*, 618–622.

(34) Andersson, K.; Malmqvist, P.-A.; Roos, B. O.; Sadlej, A. J.; Wolinski, K. *J. Phys. Chem.* **1990**, *94*, 5483–5488.

(35) Andersson, K.; Malmqvist, P.-A.; Roos, B. O. *J. Chem. Phys.* **1992**, *96*, 1218–1226.

(36) Dunning, T. H., Jr. *J. Chem. Phys.* **1989**, *90*, 1007–1023.

(37) Frisch, M. J.; Trucks, G. W.; Schlegel, H. B.; Scuseria, G. E.; Robb, M. A.; Cheeseman, J. R.; Scalmani, G.; Barone, V.; Mennucci, B.; Petersson, G. A.; et al. *Gaussian 09*, revision A.1; Gaussian, Inc.: Wallingford CT, 2009.

(38) Karlström, G.; Lindh, R.; Malmqvist, P.-Å.; Roos, B. O.; Ryde, U.; Veryazov, V.; Widmark, P.-O.; Cossi, M.; Schimmelpfennig, B.; Neogrady, P.; et al. *Comput. Mater. Sci.* **2003**, *28*, 222–239.

(39) Chapman, O. L.; Le Roux, J.-P. *J. Am. Chem. Soc.* **1978**, *100*, 282–285.

(40) Shields, C. J.; Chrisope, D. R.; Schuster, G. B.; Dixon, A. J.; Poliakov, M.; Turner, J. J. *J. Am. Chem. Soc.* **1987**, *109*, 4723–4726.

(41) (a) Li, Y.-Z.; Kirby, J. P.; George, M. W.; Poliakov, M.; Schuster, G. B. *J. Am. Chem. Soc.* **1988**, *110*, 8092–8098. (b) Tsao, M.-L.; Platz, M. S. *J. Phys. Chem. A* **2004**, *108*, 1169–1176. (c) Tsao, M.-L.; Platz, M. S. *J. Am. Chem. Soc.* **2003**, *125*, 12014–12025. (d) Gritsan, N. P.; Platz, M. S. *Chem. Rev.* **2006**, *106*, 3844–3867.

(42) Wang, J.; Burdzinski, G.; Gustafson, T. L.; Platz, M. S. *J. Org. Chem.* **2006**, *71*, 6221–6228.

(43) Wang, J.; Burdzinski, G.; Gustafson, T. L.; Platz, M. S. *J. Am. Chem. Soc.* **2007**, *129*, 2597–2606.

(44) Wang, J.; Kubicki, J.; Hilinski, E. F.; Mecklenburg, S. L.; Gustafson, T. L.; Platz, M. S. *J. Am. Chem. Soc.* **2007**, *129*, 13683–13690.

(45) Wang, J.; Burdzinski, G.; Platz, M. S. *Org. Lett.* **2007**, *9*, 5211–5214.

(46) Nibbering, E. T. J.; Elsaesser, T. *Appl. Phys. B: Laser Opt.* **2000**, *71*, 439–441.

(47) Merrick, J. P.; Moran, D.; Radom, L. *J. Phys. Chem. A* **2007**, *111*, 11683–11700.

(48) Wang, J.; Kubicki, J.; Gustafson, T. L.; Platz, M. S. *J. Am. Chem. Soc.* **2008**, *130*, 2304–2313.

(49) McClelland, R. A.; Davidse, P. A.; Hadzialic, G. *J. Am. Chem. Soc.* **1995**, *117*, 4173–4174.

(50) McClelland, R. A. *Tetrahedron* **1996**, *52*, 6823–6858.

(51) McClelland, R. A.; Kahley, M. J.; Davidse, P. A.; Hadzialic, G. *J. Am. Chem. Soc.* **1996**, *118*, 4794–4803.

(52) Davidse, P. A.; Kahley, M. J.; McClelland, R. A. *J. Am. Chem. Soc.* **1994**, *116*, 4513–4514.

(53) Montgomery, J. A.; Frisch, M. J.; Ochterski, J. W.; Petersson, G. A. *J. Chem. Phys.* **2000**, *112*, 6532–6542.

(54) Platz, M. S. In *Reactive Intermediate Chemistry*; Moss, R. A., Platz, M. S., Maitland Jones, J., Eds.; John Wiley & Sons, Inc.: Hoboken, NJ, 2004; pp 501–559.

(55) Sun, X.-Z.; Virrels, I. G.; George, M. W.; Tomioka, H. *Chem. Lett.* **1996**, 1089–1090.